HHS Public Access

Author manuscript

Nanomedicine (Lond). Author manuscript; available in PMC 2018 August 27.

Published in final edited form as:

Nanomedicine (Lond). 2014 ; 9(8): 1171–1180. doi:10.2217/nnm.13.96.

Nanowire pellicles for eukaryotic cells: nanowire coating and interaction with cells

Sung-Kyoung Kim[1], **Waeowalee Choksawangkarn**[1], **Rebecca Rose**[1], **Catherine Fenselau**[1], and **Sang Bok Lee**[*,1,2]

[1]Department of Chemistry & Biochemistry, University of Maryland, College Park, MD 20742, USA

[2]Graduate School of Nanoscience & Technology (WCU), Korea Advanced Institute of Science & Technology, Daejon, Korea

Abstract

Aim: To construct a new robust nanowire-based pellicle for eukaryotic cells, to investigate the interactions between nanowires (NWs) and cell surfaces and the internalization of nanowires, and to demonstrate for isolation of the plasma membrane with improved enrichment of transmembrane proteins.

Materials & methods: Silica NWs were coated with alumina to give positive charges on their surface. Multiple myeloma cells were coated with the positively charged NWs by dropping the cells into a buffered suspension of NWs. After the NW-coated cells were lysed, plasma membrane fragments were enriched by differential centrifugation for proteomic studies.

Results: Here we demonstrate complete cell coating with positively charged, alumina-coated silica NWs via nonspecific electrostatic interactions, and characterize a robust pellicle and little/no uptake of NWs.

Conclusion: Robust pellicles provide a new platform for therapeutic, diagnostic and biochemical interactions of nanostructures with eukaryotic cells.

Keywords

anodic aluminum oxide; cell coating; electrostatic interactions; mass spectrometry; multiple myeloma cells; nanowire; pellicles; plasma membrane; proteomics; transmembrane proteins

The interactions of nanoparticles with living cells have been widely studied in recent years, with a primary focus on delivering chemicals for therapeutics, diagnostics or imaging through internalization of the particles into the cells [1–10]. Another interesting example is the isolation of plasma membrane pellicles (or fragments) by using nanoparticle (e.g.,

*Author for correspondence: Tel.: +1 301 405 7906 slee@umd.edu.

Financial & competing interests disclosure

The research reported here was supported by a grant from the NIH (GM 021248). S-K Kim and S Bok Lee also thank the WCU program through the National Research Foundation of Korea funded by the Ministry of Education (grant number: R31–2008-000–10071-0). W Choksawangkarn acknowledges a Royal Thai Government Fellowship. We acknowledge the support of the Maryland NanoCenter and its NispLab. The NispLab is supported in part by the National Science Foundation as an MRSEC Shared Experimental Facility. The authors have no other relevant affiliations or financial involvement with any organization or entity with a financial interest in or financial conflict with the subject matter or materials discussed in the manuscript apart from those disclosed.

cationic silica nanoparticles) coating of cell surfaces to selectively separate plasma membrane proteins that are highly interesting to the proteomics community, in order to understand fundamentally how cell surface proteins change (e.g., finding marker proteins) especially when exposed to specific diseases. No satisfactory methods are currently available for enriching or isolating the plasma mem-brane [11,12]. This is a very interesting situation because the drug delivery application usually requires a high degree of nanoparticle internalization, while the plasma membrane pellicle separation with nanoparticle coating ideally requires no particle internalization into cells. Thus, an understanding of fundamental internalization behavior of nanoparticles is highly necessary, by studying interactions between nanoparticles and cells.

The construction of cell surface pellicles with nanoparticles was originally reported by Chaney and Jacobson in 1983 [13]. Their objective was to enrich the densely coated plasma membrane by differential centrifugation for biochemical analysis. This technique was first integrated with mass spectrometrybased proteomics by Rahbar and Fenselau in 2004 [14]. Since then, numerous studies have reported the use of various types of cationic nanoparticles for high-throughput profiling of the plasma membrane proteome, for example, alumina-coated silica [13,15–17], commercially available Ludox-CL aluminosilicate [14,18,19], aluminacoated iron oxide [20] and silica–magnetite nanoparticles [21,22]. It is broadly applicable to many types of samples, including attached cells, cells suspended in culture, pulmonary microvascular endothelial cells *in vivo* and hepatic sinusoidal endothelial cells *in vivo* [14–23]. Our study focuses on a fundamental of the pellicle formation with cells grown in suspension; therefore, this strategy will be applicable for analyses of the cells collected from clinical samples [23]. Previously published reports demonstrated a range of efficiency for enrichments of plasma membrane proteins using the nanoparticle pellicle technique on suspended cells. Considering the plasma membrane fraction as a percentage of the total proteins identified, based on gene ontology annotation of cellular components, a range from 18 to 42% has been reported [14,16,22,23]. One of the major problems that possibly causes contamination from cytosolic or other subcellular organelle proteins is the internalization of the nanoparticles. Another potential source of impurities is the detachment of the nanoparticles from the plasma membrane and subsequent interaction with other cellular proteins.

We report here the construction of a novel cell surface–nanowire pellicle for eukaryotic cells. Use of nanowire (NW) structure can be expected to have several benefits compared with spherical nanoparticles, such as stronger binding with the cell membrane due to multipoint interactions along the NW, thus larger membrane pellicle size for easier separation; and less cell internalization due to the larger size, thus less chance of interaction with intracellular proteins. In this paper, we systematically studied the silica NW– cell interactions with electron micrographs for each of the interaction steps in the pellicle formation process and confirmed the above hypotheses. These pellicles are constructed with short cationic silica NWs, shown schematically in Figure 1. The wire shape is hypothesized to provide higher stability and strength to the pellicles as compared with the spherical nanoparticles, owing to multiple charge interactions along the NW axis and overlapping of the NWs in the pellicles. Among many of the potential applications, we demonstrate the advantage of the NWs for plasma membrane enrichment prior to proteomic analysis.

Materials & methods

Materials

Human multiple myeloma RPMI 8226 cells and RPMI 1640 medium were purchased from American Type Culture Collection (VA, USA). Fetal bovine serum was obtained from Atlanta Biologicals (GA, USA). RC DC protein assay kits were purchased from Bio-Rad (CA, USA). Tetraethyl orthosilicate (99.999%), pen-icillin-streptomycin solution, D-sorbitol, 2-(N-mor-pholino)ethanesulfonic acid, NaCl, poly(acrylic) acid, imidazole, protease inhibitor cocktail solution, Na_2CO_3, KCl, NH_4HCO_3, urea, dithiothreitol, iodoacetamide, glutaraldehyde, Tris-HCl, beta-mercaptoethanol and sodium dodecyl sulfate were purchased from Sigma-Aldrich (MO, USA). Endoproteinase Lys-C and trypsin were purchased from Promega (WI, USA). Optima LC/MS grade acetonitrile, formic acid and trifluoroacetic acid were purchased from Thermo Fisher Scientific (PA, USA). Peptide desalting C18 TopTips™ were purchased from Glygen Corp (MD, USA). Anodic aluminum oxide (AAO) templates (Anodisc 47) with average pore diameter of approximately 200 nm and thickness of approximately 60 μm were purchased from Whatman GmbH (Dassel, Germany). Deionized water was obtained by a Milli-QA10 system (EMD Millipore Corp., MA, USA).

Synthesis of NWs

Silica NWs were synthesized through a sol-gel evaporation process according to the literature [24,25] with some modifications. Briefly, 2.08 g tetraethyl orthosilicate was added to the solution of 3.95 g ethanol and 1.8 g water followed by 3 g of 0.2 M HCl in order to make 1 M tetraethyl orthosilicate solution. The solution was hydrolyzed at 60°C for 1 h. Commercial AAO templates were immersed into the solution and then dried at room temperature for 6 h and at 120°C for 24 h, sequentially. The silica NWs were released by dissolving the templates in 25% phosphoric acid or 0.1 M sodium hydroxide. The liberated long NWs were washed several times with deionized water and then shortened by using a sonicator equipped with a microtip (Q500, Qsonica, LLC, CT, USA). Finally, the cut NWs were rinsed and stored in deionized water before use in the pellicle experiment.

The NWs were coated with an alumina layer by dis-persing the NWs in 0.01 M $Al(NO_3)_3$/ 0.1 M $K(NO_3)$ solution for 24 h. The alumina-coated NWs were dispersed in water or in a buffered solution (see below) for prompt use in cell coating experiments. The NWs were characterized by using a Hitachi SU-70 Field Emission scanning electron microscope (SEM; Hita-chi High-Technologies America Inc., MD, USA) and a JEOL JEM-2100F Field Emission transmission electron microscope (TEM; JEOL USA, Inc., MA, USA) operating at 200 kV with scanning TEM capability and Oxford energy dispersive x-ray spectrometry, and a Zetasizer Nano ZS90 particle analyzer (Malvern Instruments Ltd, Worcestershire, UK).

Cell culture & pellicle coating

RPMI 8226 human multiple myeloma cells were grown in suspension in RPMI 1640 medium supplemented with 10% fetal bovine serum and penicillin–streptomy-cin antibiotics at 37°C in a 5% CO_2 atmosphere. Cells were harvested at confluence (~6 × 107) and coated with the cationic NW suspension using a method modified from Rahbar and Fenselau [14].

The cells were collected by centrifugation at 900 ×*g* for 5 min and washed with plasma membrane-coating buffer (PMCB, 800 mM sorbitol, 20 mM 2-[N-morpholino] ethanesulfonic acid, 150 mM NaCl, pH 5.3). The cells were then applied in a dropwise fashion to excess amount of silica NWs (~5 × 1011) dispersed in PMCB, and rocked gently at 4°C for 15 min. Following removal of unbounded NWs, the NW-coated cells were placed dropwise into 10 mg/ml poly(acrylic) acid in PMCB (pH 6–6.5) and incubated with rocking at 4°C for 15 min. Excess poly(acrylic) acid was removed by sedimentation and the coated cells were washed three times in PMCB. The cells were then incubated in 2.5 mM imidazole with a protease inhibi-tor cocktail for 30 min and lysed by N_2 cavitation at 1500 or 1800 psi for 30 min. The fragments of NW-coated plasma membranes were sedimented at 100 ×*g* for 7 min, and washed three times with the lysis buffer, three times with 1 M Na_2CO_3 and three times with 1 M KCl to remove proteins that were not integral to the plasma membrane. The proteins were released from the pellicles by dissolving in 2% sodium dodecyl sulfate , 62.5 mM Tris-HCl and 5% β-mercaptoethanol at 100°C for 5 min in a microwave oven (CEM Corporation, NC, USA). Protein concentration was estimated by using an RC DC protein assay kit.

After adding cells to the NW suspension, cell coating was confirmed by optical micro scopy (Axioskop 2 MAT) with a CCD camera (AxioCam MRm; Carl Zeiss Microscopy LLC, NY, USA).

SEM sample preparation

Intact cells, NW-coated cells, poly(acrylic) acid crosslinked cells and plasma membrane pellicles were fixed with 2% glutaraldehyde in 0.12 M Millonig's phosphate buffer at pH 7.3 overnight [26]. Secondary fixation was performed using 1% OsO_4 in H_2O for 1 h. The cells were subsequently dehydrated with ethanol, ranging from 75 to 100%, and subjected to critical point drying with CO_2 using Denton DCP-1 criticalpoint dryer apparatus (Denton Vacuum, LLC, NJ, USA). The samples were coated with 15 nm of Au:Pd in a DV-503 Denton Vacuum evaporator (Denton Vacuum). SEM microscopy was performed on a Hitachi SU-70 Field Emission SEM.

Proteomic analysis

A total of 90 μg of protein was precipitated by chloroform/methanol following the published protocol [27] and resolubilized in 8 M urea in 50 mM NH_4HCO_3. Disulfide bonds were reduced in 20 mM dithiothreitol at 56°C for 30 min, and alkylation took place in 40 mM iodoacetamide in the dark for 30 min. The proteins were cleaved by endoproteinase Lys-C in 8 M urea for 3 h at 37°C, followed by trypsin cleavage in 1.6 M urea for 16 h at 37°C. The peptides were desalted using C18 TopTips following the manufacturer's procedures. The HPLC-MS/MS analysis was performed using a Shimadzu Prominent nanoHPLC (Shimadzu BioSciences, MD, USA) interfaced with an LTQ-orbitrap XL (Thermo Fisher Scientific, CA, USA). The peptides from 15 μg of proteins were injected into a Zorbax® 300SB-C18 (Agilent Technologies, CA, USA) trap column (0.3 × 5 mm) at a flow rate of 10 μl/min for 10 min, using solvent A (97.5% H_2O, 2.5% acetronitrile, 0.1% formic acid). The peptides were fractionated using a reverse-phase EVEREST® (Grace Vydac, IL, USA) C18 column (0.150 × 150 mm) with 300 Å pore size and 5 μm particle size. The flow rate was 500 nl/

min. A linear gradient was run from 5% solvent B (97.5% acetonitrile, 2.5% H_2O, 0.1% formic acid) to 40% solvent B for 120 min, and increased to 80% solvent B for 25 min. The analytical column was connected to a 15-μm fused-silica PicoTip® (New Objective, Inc., MA, USA) and interfaced with a Thermo nano-electrospray ionization source and the LTQ-orbitrap XL (Thermo Fisher Scientific). Spray voltage was set at +2 kV, and the capillary temperature was 275°C. Peptide precursor ions were measured at a resolving power set for 30,000 at m/z 400 in the orbitrap, with three averaged scans. In each activation cycle, the nine most abundant precursor ions were fragmented by collision-induced dissociation, using a normalized collision energy of 35, isolation window of 3 Da and activation time of 30 ms. Product ions were scanned in the LTQ. Ions with unassigned or +1 charge states were rejected from MS/MS scanning. Dynamic exclusion was enabled to exclude the precursor ions that were previously scanned within 3 min. Data acquisition was recorded using Xcalibur 2.0 software (Thermo Fisher Scientific, CA, USA). Replicate injections were performed to increase the identification of low abundance precursors.

Bioinformatics

Mass spectra in .RAW format were submitted to centroiding and mzXML reformatting using msconvert from ProteoWizard project [28] and searched by Pep-ArML meta-search engine [29,101]. The mass spectra were searched against a human UniprotKnowledgeBase (March 2012) with a specific tryptic cleavage. Carbamidomethylation of cysteine was set as a fixed modification and oxidation of methionine was allowed as a variable modification. The search results from seven search engines (Mascot, Tandem, OMSSA, KScore, SScore, Myrimatch and InsPecT) integrated in PepArML were filtered using in-house software. Redundant peptide identifications were removed by a global parsimony analysis. Two or more unique peptides identified with false discovery rates lower than 10% were required for each protein identification. Transmembrane proteins were assigned based on keyword information associated with the UniprotKnowledgeBase.

Results & discussion

Synthesis of silica NWs

Coating a number of cells requires the preparation of a large amount of NWs. We employed a sol-gel evaporation process for mass production of NWs. Compared with other methods, for example, solution-phase synthesis, this method is advantageous in reducing contamination caused by the use of surfactants or toxic chemicals in synthesizing NWs. Commercial AAO porous templates were immersed into precursor solutions for silica NW synthesis followed by evaporating the solution via a controlled drying process. Long NWs were collected after dissolving the AAO template to release the NWs formed in the pores of AAO (Figure 2A). The NWs had a length of approximately 60 μm, which was the thickness of the AAO template. The lengths of the NWs were varied by considering the curvature of multiple myeloma cells (as testbed eukaryotic cells for NW coating) whose diameter was approximately 10 μm, as well as voids between longer NWs attached on cell surfaces. Cutting the long NWs by using an ultrasonic probe sonicator produced NWs that were, on average, approximately 2 μm long, with the desired length distribution to fill up the voids between NWs on the cell surface (Figure 2B). The length distribution of NWs (Figure 2C)

was dependent on sonication time and intensity. It took more than 5 h at maximum intensity to shorten the silica NWs to approximately 2 μm, due to their high mechanical strength. Here, we evaluated three different lengths of silica NWs in order to study the differences in coating ability depending on varying size. Figure 2C shows the length distribution of three different silica NWs after cutting for 9 h (1.88 ± 1.77 μm), 7 h (2.17 ± 1.64 μm) and 5 h (2.49 ± 1.75 μm), respectively.

The surface of the NWs was coated with an alumina layer to give a positive charge (Figure 2D–G). The surfaces of eukaryotic cells carry negative charges due to the negatively charged phosphate group of phospholipids, which are a major component of cell membranes, as well as sialic acid moieties on surface glycoproteins. To completely coat the surface of cells, we used nonspecific electrostatic interaction of negatively charged cell surfaces with positively charged NWs. Bare silica NWs showed negative charges of approximately −40 mV in water and a slightly lower value of −35 mV in an experimental plasma membrane coating buffer at pH 5.3 (Figure 2H). We first employed silane molecules containing amine groups, for example, 3-aminopropyltriethoxysilane and (3-trimethoxysilylpropyl) diethylenetriamine, to modify silica NWs with positive charges. The values of zeta potentials, however, were quite low (~0–10 mV in both water and buffer) due to surface defects existing on silane-modified silica NWs, resulting in low binding with cell surfaces (Figure 2H) [30]. Alternatively, NWs coated with an alumina layer, revealed high positive zeta potential values (~40–50 mV in water) due to protonation of the hydrous alumina surface ($Al\text{-}OH + H^+ \leftrightarrow Al\text{-}OH_2^+$) and relatively high pI value of approximately 9 pI (Figure 2H) [31]. The highly positive surface potential value was decreased to 25–30 mV (but still very positive) when these alumina-coated silica NWs were dispersed in the coating buffer (Figure 2H). This may be explained by multivalent ions in the buffer solution, which combine with charges on the alumina surface. On the other hand, the high zeta potential values play an important role in NW dispersion, which could contribute to higher coverage of cells. Alumina-coated silica NWs had a zeta potential of approximately 50 mV in water and 30 mV in the buffer solution, which is highly promising for the formation of a uniform and robust pellicle.

NW coating & lysing cells to form membrane pellicles

Multiple myeloma cells as testbed eukaryotic cells were coated with alumina-coated NWs. Cells were dropped into a suspension of NWs in coating buffer in order to optimize contact for coating. An intact multiple myeloma cell (Figure 3A) was successfully coated with alumina-coated silica NWs (Figure 3B) after incubation for 15 min. Figure 3C shows multiple cells densely coated with the NWs. The tangled NWs on the surface of the cell reinforce the pellicle. We also looked into cellular uptake of NWs. A number of papers have reported that cellular uptake can occur with nanoparticles smaller than tens of nanometers [32–35]. In our work, the internalization of NWs will reduce the selective isolation of proteins from the plasma membrane by facilitating contamination from cytosol and organelles. Here we used NWs with a relatively large diameter of 200 nm, which reduces the internalization of NWs into cells. Figure 3D shows a TEM image of the sectioned cell, which is coated with alumina-coated silica NWs. We looked for internalization of NWs in more than 50 cells. We employed scanning TEM to obtain elemental maps to look for cellular uptake (Figure 3E & F). Figure 3G shows the only candidate we could find in over

50 cells. Red arrows point to silica NWs and Figure 3H shows the Si map. Even this image is ambiguous, however, since the cell specimen was sectioned into thin layers of approximately 100 nm, it could show a cross-section of an area mechanically caved by a long NW.

We also examined the possibility of mechanical damage (e.g., collapse and lysis) of the plasma membrane of cells with alumina-coated NWs by using optical microscopy (Figure 4). The mechanical damage of the plasma membrane may cause contamination from cytosolic and other subcellular organelle proteins due to the internalization of NWs through the damaged membrane during incubation. In our experimental process, it takes less than 1 h before the cells are fixed with 2% glutaraldehyde for electron microscopy examination. The membranes of the cells are clearly visible and circular in shape after incubation with the NWs for 70 min (Figure 4), and we conclude cautiously that coating multiple myeloma cells with alumina-coated NWs does not cause any significant mechanical damage to the cells.

We also found that the surface coverage of cells was significantly dependent on the length of NWs (Figure 5A). We prepared three different silica NWs with length distributions of 1.88 ± 1.77 μm, 2.17 ± 1.64 μm and 2.49 ± 1.75 μm. After incubation with cells, the samples were loaded on a SEM sample stage to count the number of cells completely coated with NWs. The surface coverage dramatically decreased as the length of NWs was increased. This might be attributed to the curvature of the cells. We hypothesized that NWs would have stronger interaction with cells than nanopartcles, due to binding with multiple sites on the cell surface. However, NWs longer than approximately 2 μm easily came off the cell surface. One may use longer NWs if the NWs are flexible. In this study, 1.88 ± 1.77 μm long silica NWs were found to provide optimal surface coverage. In order to test our hypothesis that NWs form strong binding with cell surfaces, NW-coated cells were lysed under high pressure and the extent of successful lysis was compared with the lysis of cells coated with spherical nanoparticles (LUDOX-CL cationic colloidal silica, average diameter of approximately 20 nm) (Figure 5B). We found that six-times as many spherical nanoparticle-coated cells were lysed at 1500 psi than NWcoated cells. NW-coated cells were lysed more completely at 1800 psi. This result indicates that multiple binding sites and overlapping NWs produce strong pellicles.

Proteomic analysis of NW pellicles

In order to confirm whether the NW pellicles allow the enrichment of plasma membranes, proteins were recovered from NW pellicles and digested with Lys-C and trypsin for LC-MS/MS analysis. Here we used cationic silica NWs that were coated with an alumina layer. Whole-cell lysate was analyzed as the control sample. We compared enrichment efficiency by evaluating identified proteins known to contain transmembrane domains as a percentage of all identified proteins. These proteins are reliably classified both experimentally and theoretically, in contrast to proteins thought to be associated with the plasma membrane in other ways [36,37]. Table 1 indicates that the use of NW pellicles doubled the identification of transmembrane proteins (11.5%) compared with those identified in whole cell lysate (5.5%). This indicates at least a twofold enrichment, but not yet a significant purification. There are several issues we are currently considering to further improve the enrichment.

First, we are trying to optimize the lysing process since we have observed quite a number of unlysed cells even after applying higher pressure of 1800 psi. Second, silica NWs may be replaced with higher density NWs, for example, iron oxide, which is expected to improve differential centrifugation.

Conclusion

NW pellicles have significant potential to provide stable pellicles for eukaryotic cells, as well as to enhance enrichment of the plasma membrane. In this study, large numbers of silica NWs were synthesized in porous AAO templates through the sol-gel evaporation process. We have successfully demonstrated complete coating of multiple myeloma cells with cationic aluminacoated silica NWs. We found that the surface coverage of cells is dependent on the length of these rigid NWs, as well as their surface charges. Notably, it was concluded, based on TEM micrographs and scanning TEM Si maps, that there is little or no internalization of NWs into cells. This is significant for applications that do not tolerate internalization of large numbers of nanoparticles. As one example of the use of such pellicles, we have demonstrated by mass spectrometrybased proteomic analysis that NW pellicles can be used to enhance enrichment of the plasma membrane.

Future perspective

Most ongoing applications of nanoparticles, for example, drug delivery, diagnostics and imaging, are based on cellular uptake of the nanoparticle carriers. On the other hand, novel applications can be envisioned that take advantage of stable nanostructures concentrated on the surface of eukaryotic cells, without internalization or cytotoxic insertion [38,39]. Recently, the Nice and Caruso groups reported a similar perspective saying “Understanding the complex and dynamic interactions between particles and biological systems is emerging as a rapidly developing scientific frontier that will provide fundamental and conceptual frameworks to improve drug carrier design for safe and effective therapy” [8]. The enrichment of plasma membrane proteins for proteomic a nalysis may be one such application.

Acknowledgements

The authors thank Y Wang, Director of Proteomic Core Facility, Maryland Pathogen Research Institute, University of Maryland, College Park, for advice with protoemic analysis; N Edwards, Department of Biochemistry and Molecular & Cellular Biology, Georgetown University, for supporting our bioinformatics; T Maugel, Director of Laboratory for Biological Ultrastructure, University of Maryland, College Park for assisting with scanning electron microscope processing.

References

Papers of special note have been highlighted as: • of interest;

• of considerable interest

1 •. Mailander V, Landfester K. Interaction of nanoparticles with cells. Biomacromolecules 10, 2379–2400 (2009).

Describes nanoparticle interactions with cell surfaces and internalization.

[PubMed: 19637907]

2. Reddy LH, Arias JL, Nicolas J, Couvreur P. Magnetic nanoparticles: design and characterization, toxicity and biocompatibility, pharmaceutical and biomedical applications. Chem. Rev 112, 5818–5878 (2012). [PubMed: 23043508]
3. Verma A, Stellacci F. Effect of surface properties on nanoparticle–cell interactions. Small 6, 12–21 (2010). [PubMed: 19844908]
4. Kobayashi H, Ogawa M, Alford R, Choyke PL, Urano Y. New strategies for fluorescent probe design in medical diagnostic imaging. Chem. Rev 110, 2620–2640 (2010). [PubMed: 20000749]
5. Son SJ, Bai X, Lee SB. Inorganic hollow nanoparticles and nanotubes in nanomedicine – part 1. Drug/gene delivery applications. Drug Discov. Today 12, 650–656 (2007). [PubMed: 17706547]
6. Son SJ, Bai X, Lee SB. Inorganic hollow nanoparticles and nanotubes in nanomedicine – part 2. Imaging, diagnostic, and therapeutic applications. Drug Discov. Today 12, 657–663 (2007). [PubMed: 17706548]
7. Nie S, Xing Y, Kim GJ, Simons JW. Nanotechnology applications in cancer. Annu. Rev. Biomed. Eng 9, 257–288 (2007). [PubMed: 17439359]
8 ••. Lai ZW, Yan Y, Caruso F, Nice EC. Emerging techniques in proteomics for probing nano-bio interactions. ACS Nano 6, 10438–10448 (2012).

Excellent perspective article discussing the use of nanoparticles for proteomic analysis.

[PubMed: 23214939]

9. Mintzer MA, Simanek EE. Nonviral vectors for gene delivery. Chem. Rev 109, 259–302 (2009). [PubMed: 19053809]
10. Overington JP, Al-Lazikzni B, Hopkins AL. How many drug targets are there? Nat. Rev. Drug Discov5, 993–996 (2006). [PubMed: 17139284]
11. Cordwell SJ, Thingholm TE. Technologies for plasma membrane proteomics. Proteomics 10, 611–627 (2010). [PubMed: 19834916]
12. Speers AE, Wu CC. Proteomics of integral membrane proteins: theory and application. Chem. Rev 107, 3687–3714 (2007). [PubMed: 17683161]
13. Chaney LK, Jacobson BS. Coating cells with colloidal silica for high yield isolation of plasma membrane sheets and identification of transmembrane proteins. J. Biol. Chem 258, 10062–10072 (1983). [PubMed: 6309765]
14. Rahbar AM, Fenselau C. Integration of Jacobson's pellicle method into proteomic strategies for plasma membrane proteins. J. Proteome Res 3, 1267–1277 (2004). [PubMed: 15595737]
15. Durr E, Yu J, Krasinska KM et al. Direct proteomic mapping of the lung microvascular endothelial cell surface *in vivo* and in cell culture. Nat. Biotechnol 22, 985–992 (2004). [PubMed: 15258593]
16. Prior MJ, Larance M, Lawrence RT et al. Quantitative proteomic analysis of the adipocyte plasma membrane. J. Proteome Res 10, 4970–4982 (2011). [PubMed: 21928809]
17. Mathias RA, Chen YS, Goode RJ et al. Tandem application of cationic colloidal silica and Triton X-114 for plasma membrane protein isolation and purification: towards developing an MDCK protein database. Proteomics 11, 1238–1253 (2011). [PubMed: 21337516]
18. Rahbar AM, Fenselau C. Unbiased examination of changes in plasma membrane proteins in drug resistant cancer cells. J. Proteome Res 4, 2148–2153 (2005). [PubMed: 16335961]
19. Li X, Xie C, Cao J et al. An *in vivo* membrane density perturbation strategy for identification of liver sinusoidal surface proteome accessible from the vasculature. J. Proteome Res 8, 123–132 (2009). [PubMed: 19053532]
20 ••. Choksawangkarn W, Kim SK, Cannon JR, Edwards NJ, Lee SB, Fenselau C. Enrichment of plasma membrane proteins using nanoparticle pellicles: comparison between silica and higher density nanoparticles. J. Proteome Res 12, 1134–1141 (2013).

Recent evaluation of alumina-coated nanoparticles for membrane protein enrichment in proteomics.

[PubMed: 23289353]

21. Zhang W, Zhao C, Wang S et al. Coating cells with cationic silica-magnetite nanocomposites for rapid purification of integral plasma membrane proteins. Proteomics 11, 3482–3490 (2011). [PubMed: 21751343]

22. Li X, Jia X, Xie C et al. Development of cationic colloidal silica-coated magnetic nanospheres for highly selective and rapid enrichment of plasma membrane fractions for proteomics analysis. Biotechnol. Appl. Biochem 54, 213–220 (2009). [PubMed: 19860738]

23. Li X, Jin Q, Cao J et al. Evaluation of two cell surface modification methods for proteomic analysis of plasma membrane from isolated mouse hepatocytes. Biochim. Biophys. Acta 1794, 32–41 (2009). [PubMed: 18707032]

24. Lu Q, Gao F, Komarneni S, Mallouk TE. Ordered SBA-15 nanorod arrays inside a porous alumina membrane. J. Am. Chem. Soc 126, 8650–8651 (2004). [PubMed: 15250707]

25. Wang D, Kou R, Yang Z, He J, Yang Z, Lu Y. Hierachical mesoporous silica wires by confined assembly. Chem. Commun 2, 166–167 (2005).

26. Millonig G Further observations on a phosphate buffer for Osmium solutions in fixation Fifth International Congress for Electron Microscopy. Breese SS, Jr (Ed.). Academic Press, NY, USA, 8 (1962).

27. Wessel D, Flugge UI. A method for the quantitative recovery of protein in dilute solution in the presence of detergents and lipids. Anal. Biochem 138, 141–143 (1984). [PubMed: 6731838]

28. Kessner D, Chambers M, Burke R, Agus D, Mallick P. ProteoWizard: open source software for rapid proteomics tools development. Bioinformatics 24, 2534–2536 (2008). [PubMed: 18606607]

29. Edwards N, Wu X, Tseng TW. An unsupervised, model-free, machine-learning combiner for peptide identifications from tandem mass spectra. Clin. Proteomics 5, 23–36 (2009).

30. Metwalli E, Haines D, Becker O, Conzone S, Pantano CG. Surface characterization of mono-, di-, and tri-aminosilane treated glass substrates. J. Colloid Interf. Sci. 298, 825–831 (2006).

31. Perrott KW. Surface charge characteristics of amorphous aluminosilicates. Clay. Miner 25, 417–421 (1997).

32. Albanese A, Tang PS, Chan WCW. The effect of nanoparticle size, shape, and surface chemistry on biological systems. Annu. Rev. Biomed. Eng 14, 1–16 (2012). [PubMed: 22524388]

33. Gratton SEA, Ropp PA, Pohlhaus PD et al. The effect of particle design on cellular internalization pathways. Proc. Natl Acad. Sci. USA 105, 11613–11618 (2008). [PubMed: 18697944]

34 •. Nan A, Bai X, Son SJ, Lee SB, Ghandehari H. Cellular uptake and cytotoxicity of silica nanotubes. Nano Lett. 8, 2150–2154 (2008).

Cytotoxicity and internalization mechanism of nanowirelike silica nanoparticles.

[PubMed: 18624386]

35. Chithrani BD, Chan WCW. Elucidating the mechanism of cellular uptake and removal of protein-coated gold nanoparticles of different sizes and shapes. Nano Lett. 7, 1542–1550 (2007). [PubMed: 17465586]

36. Elschenbroich S, Kim Y, Medin JA, Kislinger T. Isolation of cell surface proteins for mass spectrometry-based proteomics. Expert Rev. Proteomics 7, 141–154 (2010). [PubMed: 20121483]

37. Speers AE, Wu CC. Proteomics of integral membrane proteins – theory and application. Chem. Rev 107, 3687–3714 (2007). [PubMed: 17683161]

38. Buyukserin F, Medley CD, Mota MO et al. Antibodyfunctionalized nano test tubes target breast cancer cells. Nanomedicine (Lond.) 3, 283–292 (2008). [PubMed: 18510424]

39. Hillebrenner H, Buyukserin F, Stewart JD, Martin CR. Template synthesized nanotubes for biomedical delivery applications. Nanomedicine (Lond.) 1, 39–50 (2006). [PubMed: 17716208]

101. PepArML Meta-Search Engine. https://edwardslab.bmcb.georgetown.edu/pymsio

Executive summary

- Large numbers of silica nanowires (NWs) were synthesized in porous anodic aluminum oxide templates through the sol-gel evaporation process.
- Complete coating of multiple myeloma cells was achieved with cationic alumina-coated silica NWs, with strong binding and little/no internalization.
- The surface coverage of eukaryotic cells is dependent on the length of NWs as well as surface charge.
- Proteomic analysis confirmed that NW pellicles enhance the enrichment of transmembrane proteins in the plasma membrane. We are currently evaluating various NWs to optimize this enrichment.

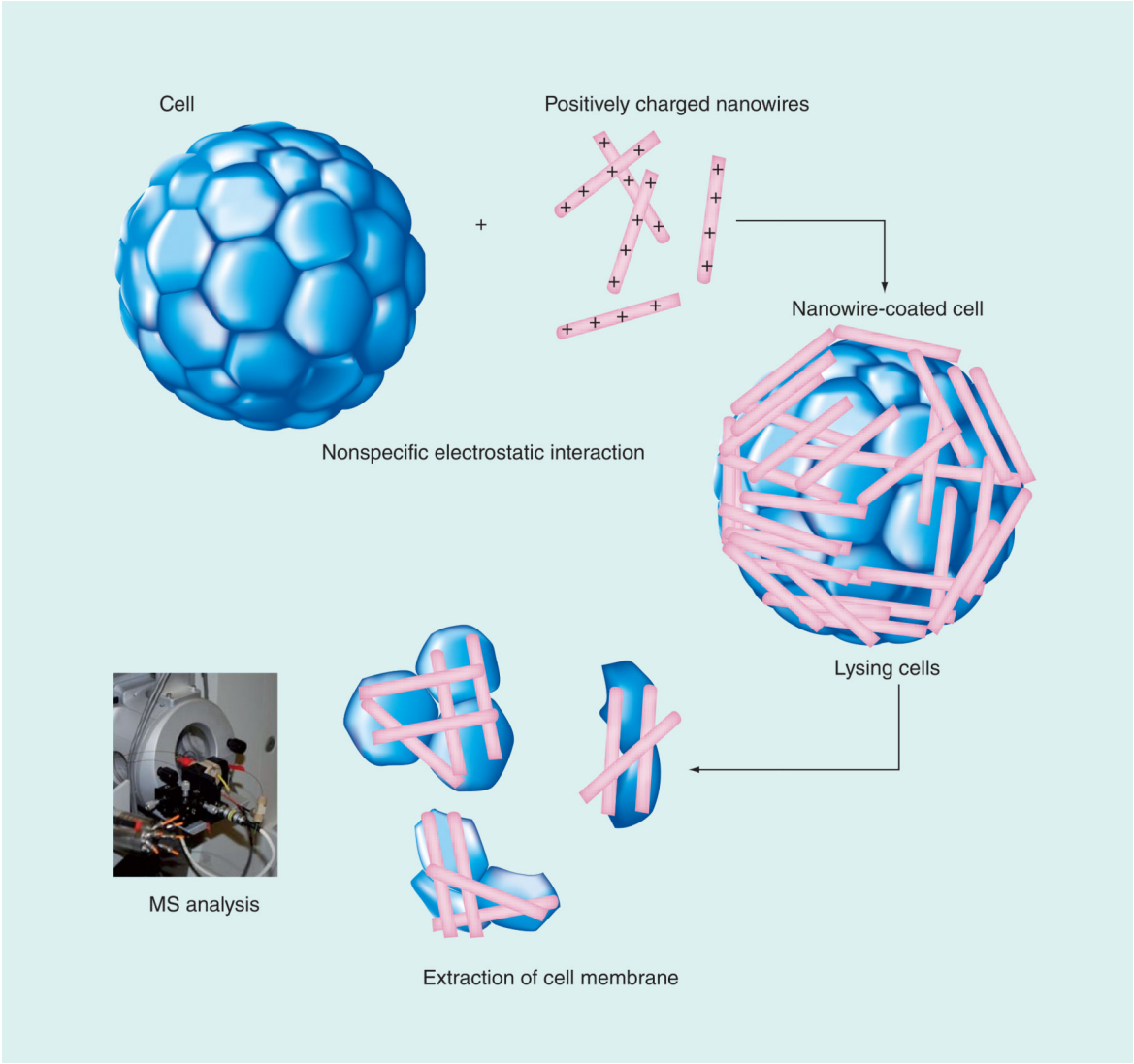

Figure 1. Process of coating cells with positively charged nanowires.

Multiple myeloma cells with a negatively charged surface are incubated with positively charged nanowires in order to coat cell surfaces with nanowires through nonspecific electrostatic interaction. After lysing the cells under high pressure, the plasma membrane fragments supported on nanowire pellicles are isolated by centrifugation. MS is employed to analyze plasma membrane proteins.

MS: Mass spectrometry.

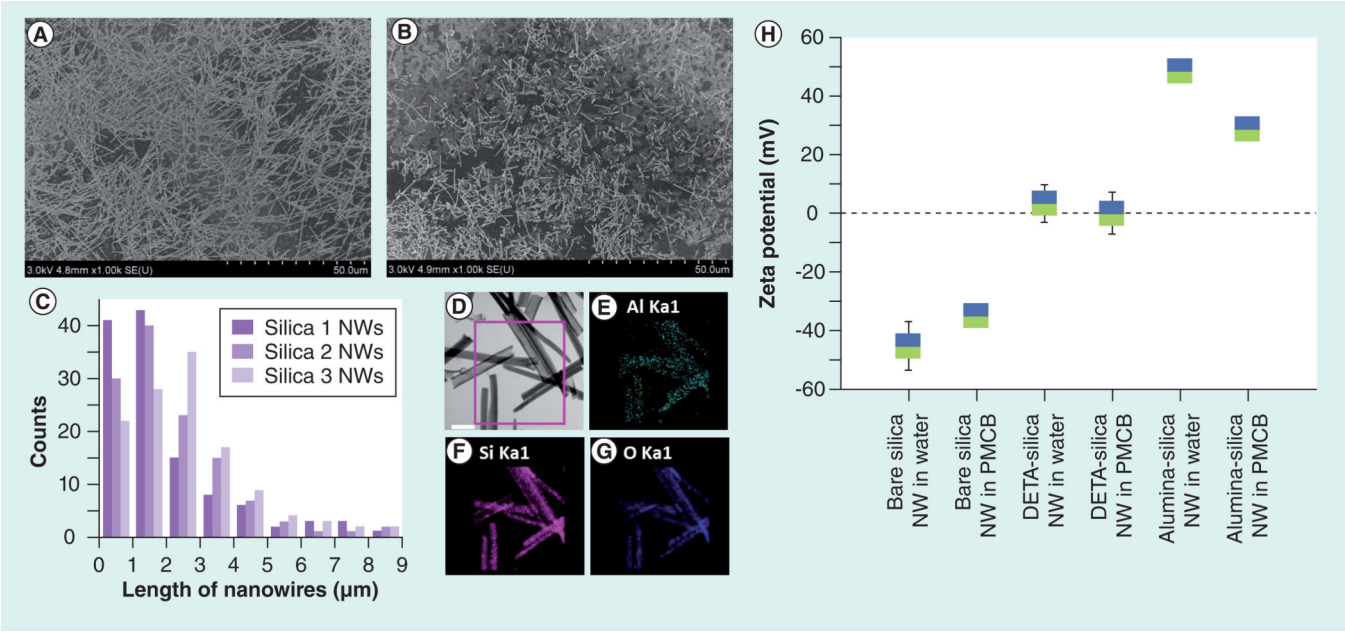

Figure 2. Scanning electron microscope images of silica nanowires and their zeta potential values with various surface modifications.

(A) After dissolving anodic aluminum oxide templates and **(B)** after cutting the NWs by sonication. **(C)** Length distribution of silica NWs after cutting for 9 h (silica 1 NWs), 7 h (silica 2 NWs) and 5 h (silica 3 NWs). **(D)** Transmission electron microscope image of silica NWs and energy dispersive x-ray spectroscopy mapping of **(E)** Al, **(F)** Si and **(G)** O. **(H)** Zeta potential values of bare, (3-trimethoxysilylpropyl) DETA-modified and alumina-modified silica NWs in water and PMCB.

DETA: Diethylenetriamine; NW: Nanowire; PMCB: Plasma membrane-coating buffer.

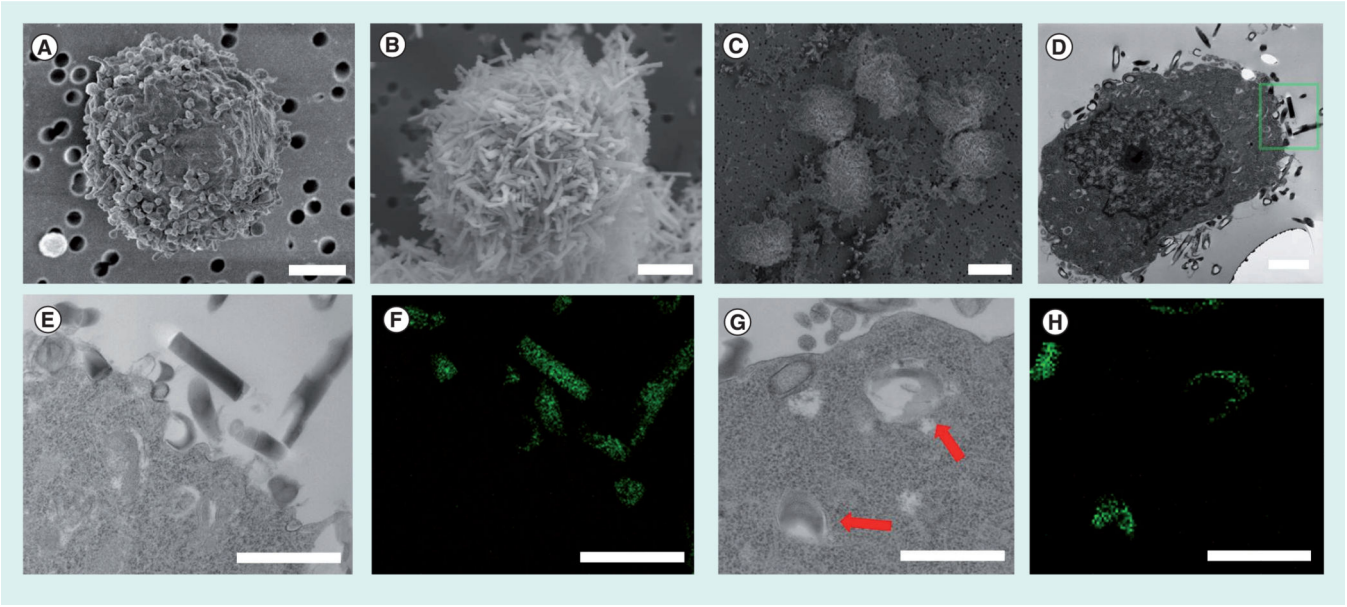

Figure 3. Scanning electron microscope and transmission electron microscope images of multiple myeloma cells.

(A) Intact cell, **(B)** cell coated with alumina-coated silica nanowires (NWs) and **(C)** multiple cells on a polymer membrane after coating with silica NWs. **(D)** Transmission electron microscope image of a cell coated with alumina-coated silica NWs, **(E & F)** magnified image of the rectangular area in **(D)** and elemental mapping of Si by scanning transmission electron microscope and **(G & H)** transmission electron microscope image of a cell coated with NWs and its Si mapping. The scale bars are 2 μm in **(A & B)**, 10 μm in **(C)**, 1 μm in **(D & F)**, and 500 nm in **(G & F)**.

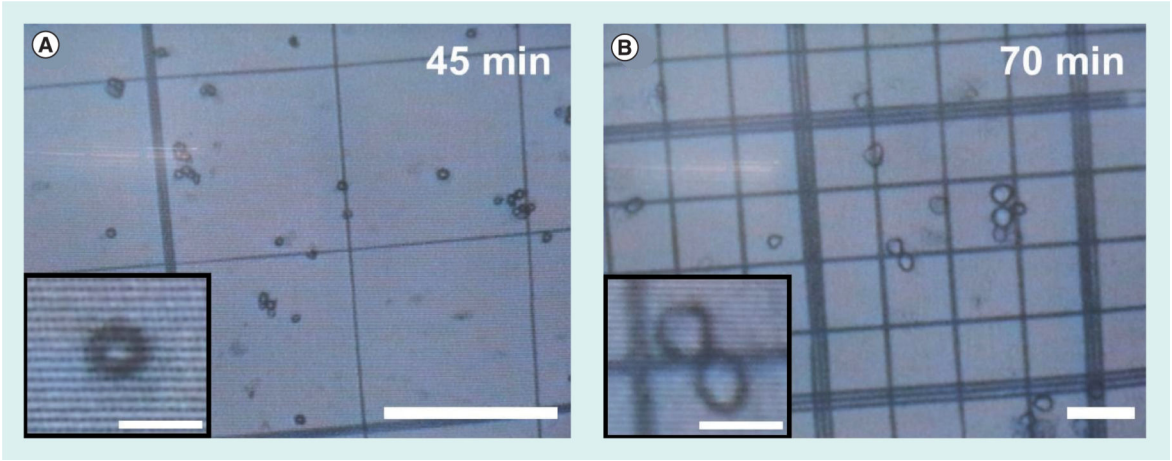

Figure 4. Optical microscope images of multiple myeloma cells aged for two different intervals after coating with silica nanowires.

The cell membranes are clearly visible and circular after coating with nanowires. The optical images of cells are not disrupted by coating with alumina-coated silica nanowires since silica has a refractive index similar to water and to the glass slide. The insets show the magnified images of cells. The scale bars are 100 μm for **(A)**, 25 μm for **(B)** and 10 μm for the insets.

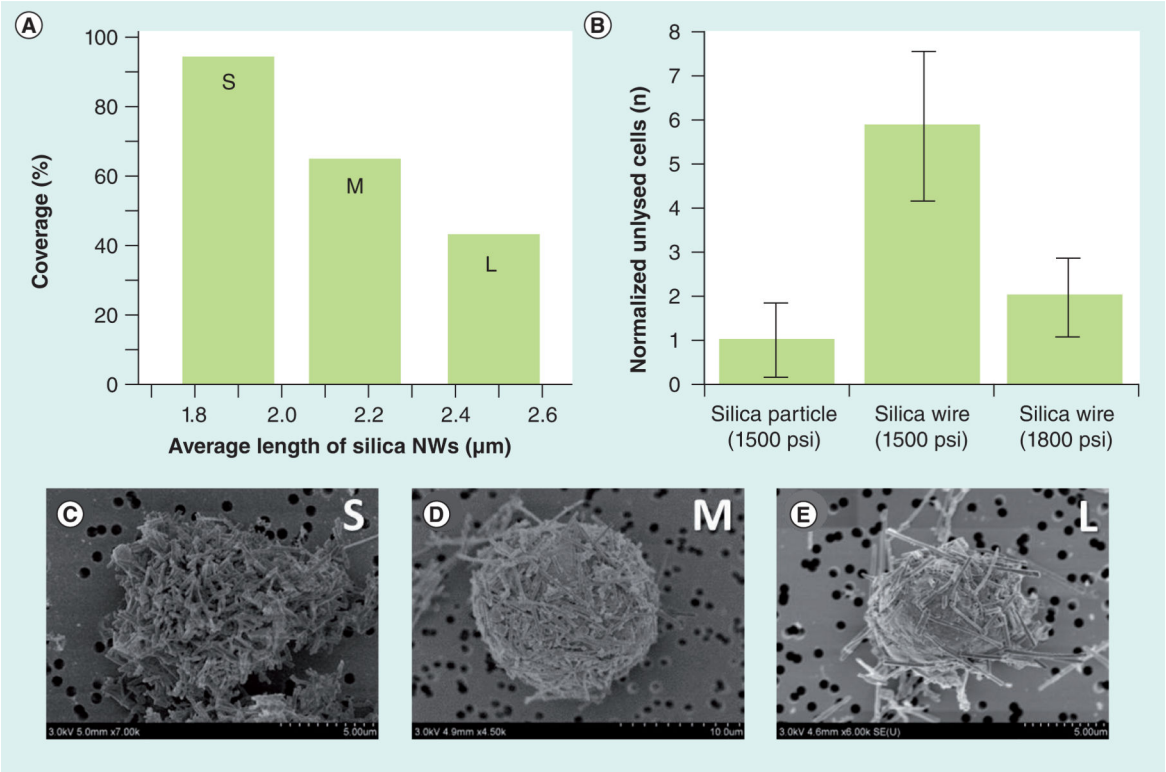

Figure 5. Surface coverage of cells by nanowires coating and number of unlysed cells observed after lysis.

(A) Variation of surface coverage of multiple myeloma cells with the length of alumina-coated silica NWs. Each S, M and L has ±15% deviation in maximum. **(B)** Normalized number of unlysed cells after lysing the cells coated with alumina-coated silica particles and NWs under high pressures. **(C–E)** Representative scanning electron microscope images of the cells coated with different lengths of NWs. **(C)** A cell coated with an average length of silica NWs referred to as S in **(A)**; **(D)** a cell coated with NWs referred to as M in **(A)**; **(E)** a cell coated with NWs referred to as L in **(A)**.

NW: Nanowire.

Table 1.

Proteomic analysis of silica nanowire-coated cell pellicles.

Type of cells	Transmembrane proteins, % (standard deviation)
Silica NW-coated cells	11.5 (0.7)
Intact cells	5.5 (1.2)

NW: Nanowire.